ELSEVIER

Composites: Part B 32 (2001) 503–511

composites
Part B: engineering

www.elsevier.com/locate/compositesb

On stiffness properties of square honeycombs and other unidirectional composites

Stein A. Berggren[a], Dag Lukkassen[b,*], Annette Meidell[a], Leon Simula[c]

[a]Narvik University College, HiN, N-8505 Narvik, Norway
[b]Narvik University College and Norut Technology Ltd, N-8505 Narvik, Norway
[c]Narvik University College and Natech Ltd, N-8505 Narvik, Norway

Received 14 March 2001; accepted 25 May 2001

Abstract

In this paper we consider stiffness properties of square symmetric unidirectional two-phase composites with given volume fractions. First, we compare the effective moduli of the stiffest possible (or softest possible) of such materials which satisfy transverse isotropy or square isotropy with that of materials satisfying 3D-isotropy.

Next, we present some numerical FEM computations of in-plane stiffness properties of square honeycombs. Our results are compared with the effective moduli of the stiffest possible square symmetric composites. The numerical results are used to optimize the directions of square prisms in the core of sandwich plates with respect to stiffness. Our calculations can therefore be useful in connection with optimization of structural topology. © 2001 Published by Elsevier Science Ltd.

Keywords: A. Fibers; A. Honeycomb; B. Elasticity; A. Plates; Stiffness

1. Introduction

Engineering and mathematical aspects of the homogenization method for determination of effective properties of composites have been discussed in several papers and books, see e.g. Refs. [5,11,14,20,24] (for other methods, e.g. discrete network analysis, see Ref. [9]).

In this paper, we consider stiffness properties of square symmetric unidirectional two-phase composites with given volume fractions. First, we compare the effective moduli of the stiffest possible (or softest possible) of such materials which satisfy transverse or square isotropy with that of materials satisfying 3D-isotropy. Our comparison is based on a rewritten version of some optimal bounds for such materials. The main result of this comparison is presented in Remarks 4–9.

Next, we present some numerical FEM computations of in-plane stiffness properties of square honeycombs. Special attention is payed to the accuracy of the computations by comparing our FEM-results with results obtained by using the method of Greengard and Helsing [10]. Our results are compared with the effective moduli of the stiffest possible square symmetric composites. The main observation concerning these numerical calculations is that the in-plane stiffness properties of square honeycombs turn out to be less than expected. The numerical results are used to optimize the directions of square prisms in the core of sandwich plates with respect to stiffness. The observed tendencies in our numerical results are discussed and also explained by use of simple illustrations. It also seems that our calculations can be useful in connection with the optimization of structural topology (see [4]).

The paper is organized as follows. In Section 2, we discuss and compare some bounds for effective properties. We consider numerical computations of square honeycombs in Section 3. Section 4 is left for some final comments and concluding remarks. All the numerical values can be found in Appendix A.

2. On bounds for effective elastic properties

A precise definition of the effective moduli in general can be found elsewhere (see e.g. Ref. [2]). Therefore, we will not go into details here.

Let us consider the case of two-component unidirectional fiber composites with local shear moduli $G_1 < G_2$ and local plane strain bulk moduli $K_1 < K_2$ with corresponding volume fractions p_1 and p_2. In addition, assume that the

* Corresponding author.
E-mail address: Dag.Lukkassen@hin.no (D. Lukkassen).

1359-8368/01/$ - see front matter © 2001 Published by Elsevier Science Ltd.
PII: S1359-8368(01)00029-4

composite satisfies the property of square symmetry, i.e. that the effective stiffness matrix for the plane strain problem is of the form

$$\begin{bmatrix} K^* + G_T^* & K^* - G_T^* & 0 \\ K^* - G_T^* & K^* + G_T^* & 0 \\ 0 & 0 & G_{T,45}^* \end{bmatrix},$$

where K^* is the effective transverse bulk modulus and G_T^* and $G_{T,45}^*$ are the effective transverse shear moduli. Then, it is possible to prove the following bounds for the effective bulk modulus K^*:

$$p_1K_1 + p_2K_2 - \frac{p_1p_2(K_1 - K_2)^2}{p_2K_1 + p_1K_2 + G_1} \le K^* \le p_1K_1 + p_2K_2 - \frac{p_1p_2(K_1 - K_2)^2}{p_2K_1 + p_1K_2 + G_2}, \tag{2.1}$$

the following bounds for the effective transverse shear moduli G_T^* and $G_{T,45}^*$:

$$\left(G_1^{-1}p_1 + G_2^{-1}p_2\right)^{-1} \le G_T^*, G_{T,45}^* \le p_1G_1 + p_2G_2 - \frac{p_1p_2(G_1 - G_2)^2}{p_2G_1 + p_1G_2 + K_2}, \tag{2.2}$$

and the following bounds for the effective longitudinal shear modulus G_L^* :

$$p_1G_1 + p_2G_2 - \frac{p_1p_2(G_1 - G_2)^2}{p_2G_1 + p_1G_2 + G_1} \le G_L^* \le p_1G_1 + p_2G_2 \frac{p_1p_2(G_1 - G_2)^2}{p_2G_1 + p_1G_2 + G_2}. \tag{2.3}$$

Concerning these facts and some further information, see Refs. [1,7,8,11,14]. Moreover, by Hill [13] we have the following bounds for the effective longitudinal Young's modulus E_L^* and the effective longitudinal Poisson's ratio ν_L^* :

$$\frac{p_1p_2}{(p_1/K_2) + (p_2/K_1) + (1/G_1)} \le \frac{E_L^* - p_1E_1 - p_2E_2}{4(\nu_1 - \nu_2)^2} \le \frac{p_1p_2}{(p_1/K_2) + (p_2/K_1) + (1/G_2)},$$

$$\frac{p_1p_2}{(p_1/K_2) + (p_2/K_1) + (1/G_1)} \le \frac{\nu_L^* - p_1\nu_1 - p_2\nu_2}{(\nu_1 - \nu_2)(1/K_2 - 1/K_1)} \le \frac{p_1p_2}{(p_1/K_2) + (p_2/K_1) + (1/G_2)},$$

where E_i and ν_i are Young's modulus and Poisson's ratio, respectively, of the phase.

Remark 1. The latter two bounds were proved in Ref. [13] for the case of transverse isotropy. However, by following the proof in Ref. [13] it is easy to check that the same facts hold in the case square isotropy.

Remark 2. It is interesting to note that the longitudinal Young's modulus E_L^* is always larger (or equal to) the arithmetic mean of the local Young's modulus $p_1E_1 + p_2E_2$. We may even have that E_L^* is larger than $\max\{E_1, E_2\}$, which shows that E_L^* is not any type of mean of E_1, E_2 (note that a mean of numbers always lies between the minimum and maximum, see Ref. [3, p. 35 Remark 5]). As an example put $p_1 = p_2 = 1/2$, $E_1 = E_2$ and $\nu_1 = 0$, $\nu_2 = \frac{1}{2}$ (like cork and rubber, respectively). In this case, E_L^* turns out to be 7.9% larger than $E_1 = E_2$ for the most extreme structure.

If we in addition assume that $G_T^* = G_{T,45}^*$ (i.e. plane isotropy) we obtain the same bounds for K^* and G_L^* but the following sharper bounds for G_T^* :

$$p_1G_1 + p_2G_2 - \frac{p_1p_2(G_1 - G_2)^2}{p_2G_1 + p_1G_2 + G_{1\#}} \le G_T^* \le p_1G_1 + p_2G_2 - \frac{p_1p_2(G_1 - G_2)^2}{p_2G_1 + p_1G_2 + G_{2\#}}, \tag{2.4}$$

where

$$G_{1\#} = \frac{K_1G_1}{K_1 + 2G_1}, \qquad G_{2\#} = \frac{K_2G_2}{K_2 + 2G_2}.$$

On the other hand, if we assume that the composite macroscopically is isotropic in the three dimensional sense (not unidirectional fibers), then we obtain the following bounds for the effective three dimensional bulk modulus $k^*(= K^* - G^*/3)$ and the effective shear modulus G^*:

$$p_1k_1 + p_2k_2 - \frac{p_1p_2(k_1 - k_2)^2}{p_2k_1 + p_1k_2 + k_{1\#}} \le k^* \le p_1k_1 + p_2k_2 - \frac{p_1p_2(k_1 - k_2)^2}{p_2k_1 + p_1k_2 + k_{2\#}} \tag{2.5}$$

and

$$p_1G_1 + p_2G_2 - \frac{p_1p_2(G_1 - G_2)^2}{p_2G_1 + p_1G_2 + G_{1\#}} \le G^* \le p_1G_1 + p_2G_2 - \frac{p_1p_2(G_1 - G_2)^2}{p_2G_1 + p_1G_2 + G_{2\#}}, \tag{2.6}$$

where

$$k_i = K_i - \frac{G_i}{3}, \qquad k_{i\#} = \frac{4}{3}G_i$$

and

$$G_{i\#} = G_i\frac{8G_i + 9k_i}{6(2G_i + k_i)}$$

(more generally in dimension n:

$$k_i = K_i + \frac{(2-n)G_i}{n},$$

$$k^* = K^* + \frac{(2-n)G^*}{n},$$

$$k_{i\#} = \frac{2(n-1)}{n}G_i,$$

$$G_{i\#} = G_i\frac{2G_i(n^2-n-2)+k_in^2}{2n(2G_i+k_i)}.\Big)$$

The bounds (2.5) and (2.6) are the same bounds as those presented in Jikov et al. [16], but rewritten in a different and perhaps more convenient way (especially in view of the discussion below).

Remark 3. All the above bounds are best possible, i.e. there exist structures such that the bounds are attained.

Noting that (for $n = 3$)

$$G_{i\#} = G_i\frac{8G_i+9k_i}{6(2G_i+k_i)} = G_i\frac{8G_i+9(K_i-(G_i/3))}{6(2G_i+(K_i-(G_i/3))}$$

$$= G_i\frac{5G_i+9K_i}{2(5G_i+3K_i)},$$

we obtain that the upper bound for the shear modulus given in Eq. (2.6) is less than the upper bound given in Eq. (2.2) when

$$G_i\frac{5G_i+9K_i}{2(5G_i+3K_i)} \le K_i \tag{2.7}$$

for $i = 2$, i.e.

$$(K_i+G_i)(6K_i-5G_i) \ge 0,$$

and since $K_i, G_i > 0$, we obtain that $6K_i - 5G_i \le 0$. Thus,

$$6K_i \ge 5G_i$$

or equivalently

$$\frac{6E_i}{2(1+\nu_i)(1-2\nu_i)} \ge \frac{5E_i}{2(1+\nu_i)}$$

(recall the well-known relations: $K_i = (E_i/2(1+\nu_i)\times(1-2\nu_i))$ and $G_i = E_i/2(1+\nu_i)$). Hence, we make the following interesting conclusions:

Remark 4. The upper bound for the shear modulus is the three-dimensional isotropic case given in Eq. (2.6) is less than the upper bound in the square symmetric case given in Eq. (2.2) if and only if $\nu_2 \ge -0.1$, which normally is satisfied since 'natural' materials almost always possess positive Poisson's ratios (however there exist materials with negative Possion's ratios, see e.g. Refs. [17,23]).

Remark 5. Since $G_1, G_{1\#} > 0$, and since the lower bound of Eq. (2.2) can be written

$$p_1G_1 + p_2G_2 - \frac{p_1p_2(G_1-G_2)^2}{p_2G_1+p_1G_2+0},$$

we have that the lower bound for the shear modulus is smallest for the square symmetric case given in Eq. (2.2).

Remark 6. Since

$$\frac{K_iG_i}{K_i+2G_i} \le G_i\frac{5G_i+9K_i}{2(5G_i+3K_i)},$$

we always have that the bounds for the shear modulus in the plane isotropic case given in Eq. (2.4) are less than the bounds for the three-dimensional isotropic case (2.6).

Remark 7. By replacing the right side of Eq. (2.7) with G_i we obtain similarly that the lower bound (resp. upper bound) for the shear modulus in the three-dimensional isotropic case given in Eq. (2.6) is less than the lower bound (resp. upper bound) for the longitudinal shear modulus in the square symmetric case given in Eq. (2.3) if and only if $\nu_1 \le 0.2$ (resp. $\nu_2 \le 0.2$).

Remark 8. Since $G_2 < K_2$ for positive Poisson's ratios we have that the upper bound for the longitudinal shear modulus in the square symmetric case given in Eq. (2.3) is less than the upper bound for the transverse shear moduli given in Eq. (2.2) if and only if $\nu_2 > 0$.

Remark 9. Since

$$\frac{K_iG_i}{K_i+2G_i} + \le G_i,$$

we always have that the bounds for the shear modulus in the plane isotropic case given in Eq. (2.4) are less than the

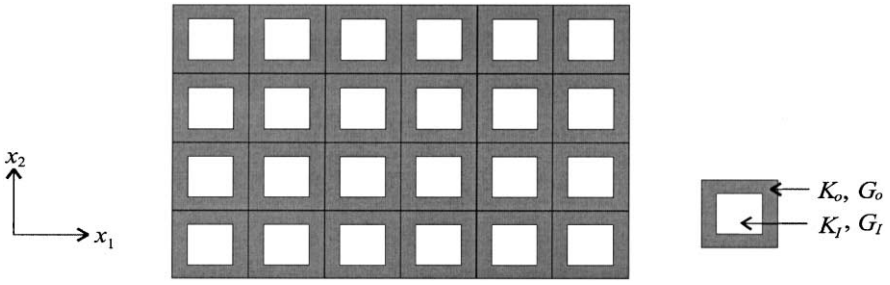

Fig. 1. The square honeycomb structure.

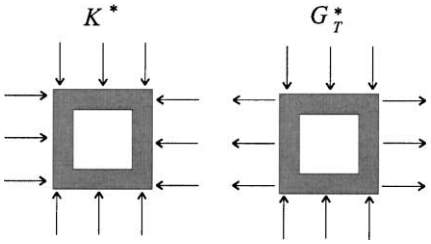

Fig. 2. The two effective moduli measure resistance against the indicated average strains.

bounds for the longitudinal shear modulus in the square symmetric case given in Eq. (2.3).

3. Numerical calculations of the effective moduli for square honeycombs

We consider the case of square honeycombs with locally isotropic material properties (see Fig. 1) where $K_I < K_0$ and $G_I < G_0$. In order to compare with the upper bounds of Eqs. (2.2) and (2.1) we have computed K^* and G_T^* numerically by solving the cell problem on a quarter of a period of the structure (see Fig. 3). For details concerning the method of computing the effective elastic moduli in general, see e.g. Refs. [2,5,10,12,14,20,24]. A visual interpretation of K^* and G_T^*, is given in Fig. 2. The numerical procedure used in this paper follows the one presented in Ref. [2] which is a variant of those used earlier in [14,20,24]. We do not compute $G_{T,45}^*$ since this value often is significantly less than G_T^* and therefore very far from the upper bound of Eq. (2.2).

The values of these moduli computed numerically by a FEM-program are always larger than the exact value. This follows by the fact that the exact effective moduli turn out to be the minimum of a variational problem taken over a function space. Concerning this fact see Ref. [16] (for an analogy to the heat conduction problem see Refs. [21,22]).

Let K^{*+} and G_T^{*+} denote the (FEM) numerical values of K^* and G_T^*. Moreover, let error K^{*+} and error G_T^{*+} denote the corresponding maximum error estimate for our calculations using the method developed in Ref. [6] (used for the estimation of the error in calculating the strain energy in case of even more general boundary conditions). Since K^* and G_T^* are minimum values of some variational problems it follows that

$$K^{*-} \le K^* \le K^{*+}$$

$$G_T^{*-} \le G_T^* \le G_T^{*+},$$

where $K^{*-} = K^{*+} - \text{error } K^{*+}$ and $G_T^{*-} = G_T^{*+} - \text{error } G_T^{*+}$. Consider also the maximum error estimates in %

$$\text{me } K^* = \frac{\text{error } K^{*+}}{K^{*-}} 100,$$

$$\text{me } G_T^* = \frac{\text{error } G_T^{*+}}{G_T^{*-}} 100.$$

Furthermore, let d_{K^*} and $d_{G_T^*}$ denote the difference in % between K^* and the upper bound K_{HS+}^* in Eq. (2.1) and between G_T^* and the upper bound G_{HS+}^* in Eq. (2.2), i.e.

$$d_{K^*} = \frac{K_{HS+}^* - K^{*+}}{K^{*+}} 100,$$

$$d_{G_T^*} = \frac{G_{HS+}^* - G_T^{*+}}{G_T^{*+}} 100.$$

In the table presented in Appendix A, we have listed K^*/K_0, me K^*, d_{K^*}, G^*/G_0, me G_T^* and $d_{G_T^*}$ for some values of the volume fraction p_I and the Poisson's ratio ν_0 for the case when the Young's modulus of the inner material is negligible. We have used quadrilateral-solid elements. Each element has eight nodes, and each node has two degrees of freedom (the values of the displacements in the x_1- and x_2- direction). See Fig. 3, which shows the triangulation for the case $p_I = 0.8$.

An effort has been made to obtain accurate computations. For some cases, we have compared our FEM-results with results obtained with a fast multipole-accelerated iterative scheme based on integral equations and developed by Greengard and Helsing [10] (see Ref. [12] for details on the particular implementation). Using sufficiently long computation time the method of Greengard and Helsing ensures error less than 10^{-10}%. In all the cases that we have tested it turns out that the maximum error estimates me K^* and me G_T^* are much larger than the actual error. This indicates that out table-values for d_{K^*} and $d_{G_T^*}$ probably are considerably more accurate than estimated (see also Ref. [6] for similar considerations).

The calculation has been performed by using the FEM-code ANSYS.

4. Some final comments and concluding remarks

From the table in Appendix A, we observe that the effective bulk modulus K^* of square honeycombs becomes

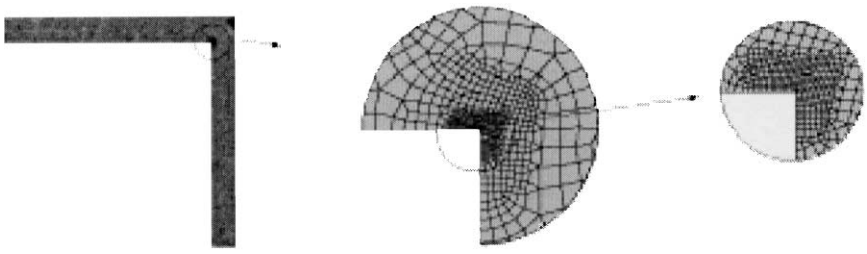

Fig. 3. The FEM-model of a quarter of a period of the structure.

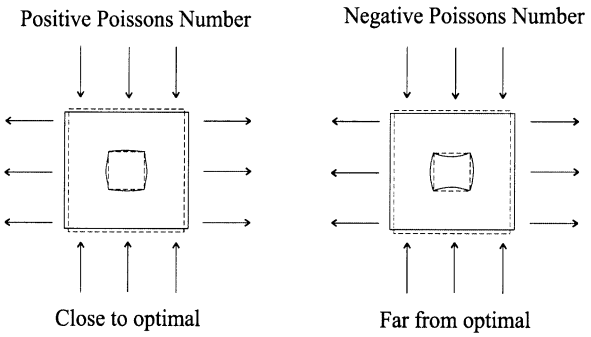

Fig. 4. Deformation related to the computation of the shear modulus G_T^*.

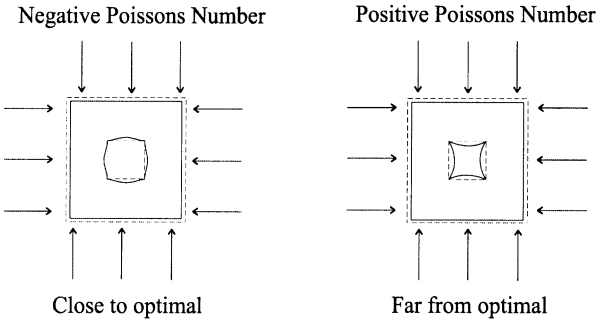

Fig. 5. Deformation related to the computation of the bulk modulus K^*.

relatively closer to the upper bound K_{HS+}^* in Eq. (2.1) as the Poisson's ratio increases. On the other hand, we observe that the effective shear modulus G_T^* becomes relatively closer to the upper bound G_{HS+}^* in Eq. (2.2) as the Poisson's ratio decreases. These tendencies are particularly apparent for small values of p_I (see e.g. Appendix A). Figs. 4 and 5 may help to explain this behavior since it is reasonable to think (but not obvious) that the objects to the left could have been made more resistant against the indicated effective strains than those to the right.

The values of d_{K^*} and $d_{G_T^*}$ turn out to be somewhat larger than we expected. By iterating square honeycombs it has

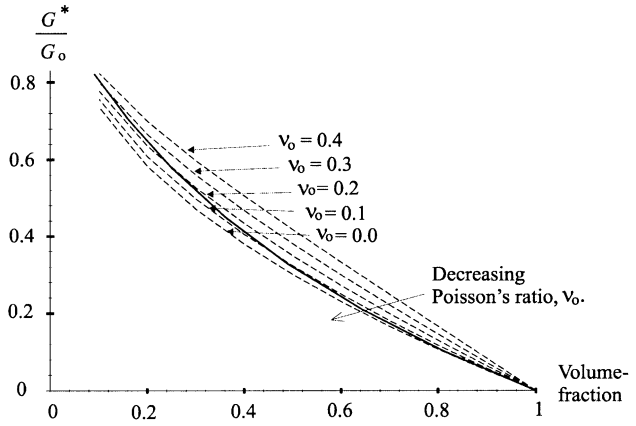

Fig. 7. Plots for G_T^*/G_o (dotted lines) and G_L^*/G_o (solid line).

been proven that it is possible to make K^*, G_T^* and G_L^* as close as we want to the upper bounds of Eqs. (2.1)–(2.3), respectively (see Ref. [19]). Moreover for square honeycombs it turns out that G_L^* is relatively close to the corresponding upper bound in Eq. (2.3). Thus one could expect that this also would be the case for K^* and G_T^*. However, this is not true. For example, for $p_I = 0.1$ we have that the deviation between G_L^* and the upper bound $d_{G_L^*} = 1.7\%$ (see Ref. [21]). On the other hand, we observe from Appendix A that the corresponding values for the bulk modulus and shear modulus are up to 12.2 and 18.6%, respectively. Moreover, the highest possible value for $d_{G_L^*}$ is 4.6% whereas the highest value for d_{K^*} and $d_{G_T^*}$ are 15.4 and 21.7%, respectively.

By interpolating the table values it is possible to obtain very accurate values of K^* and G_T^* for any value of p_I and the local moduli K_o and G_o (or E_o and ν_o). This may be useful e.g. in connection with optimization of structural topology and material (see Ref. [4]).

Square honeycombs can be used as cores in sandwich panels. One of the primary functions of the honeycomb cores is to carry the shear loads in the panel surface.

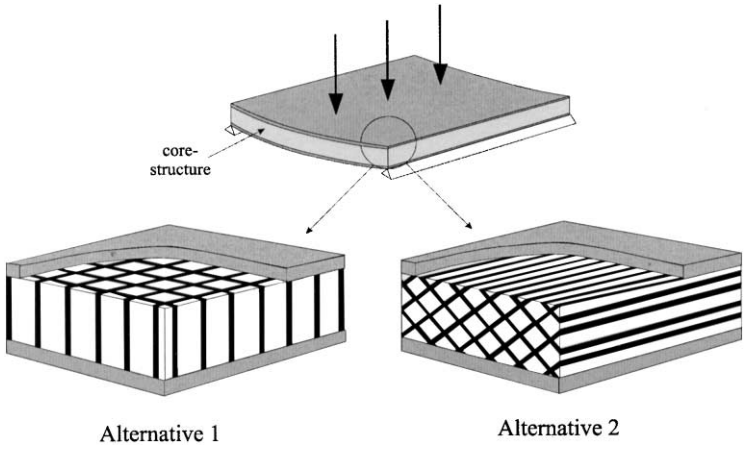

Fig. 6. Sandwich plate with two alternative cores.

When the axis of the square prisms is perpendicular to the panel surface (see Alternative 1 in Fig. 6) the shear strain resistance in the core is given by the longitudinal shear modulus G_L^* in both orthogonal directions in the panel plane. On the other hand, when the axis of the square prisms is parallel with the panel surface (see Alternative 2 in Fig. 6) the shear strain resistance in the core will be given by the transverse shear modulus G_T^* in one direction in the panel plane and by the longitudinal shear modulus G_L^* in the other direction. What alternative which is best will therefore depend on whether G_T^* is larger or less than G_L^*. The latter will depend on the volume fraction of the core p_I and the Poisson's ratio ν_o. By using our numerical calculations, we have plotted G_T^*/G_o for some values of Poisson's ratio ν_o in Fig. 7. In the same figure we have also plotted G_T^*/G_o (the solid line), borrowed from Ref. [21]. Now, using Fig. 7 we can easily find the best alternative. The results can be summed up in the following table: ([1]depending on the volume fraction p_I)

Poisson's ratio, ν_o	≤ 0.0	0.1	0.2	0.3	0.4
Alternative 1	Stiffest	Stiffest/softest[1]	Stiffest/softest[1]	Softest	Softest
Alternative 2	Softest	Stiffest/softest[1]	Stiffest/softest[1]	Stiffest	Stiffest

Acknowledgements

The authors thank three anonymous referees for some valuable comments which have improved the presentation of this paper.

Appendix A

	ν_o	K^*/K_o	me K^* (%)	d_{K^*} (%)	G^*/G_o	me G_T^* (%)	$d_{G_T^*}$ (%)
$p_I = 0.1$							
	−0.95	0.8456792	0.018	2.9	0.5883600	0.00152	18.6
	−0.9	0.8444856	0.019	2.9	0.5946380	0.00149	18.2
	−0.8	0.8418332	0.019	3.0	0.6076020	0.00142	17.6
Number of elements: 5763	−0.7	0.8387640	0.019	3.0	0.6211410	0.00135	16.9
	−0.6	0.8351614	0.020	3.1	0.6353000	0.00128	16.1
	−0.5	0.8308800	0.021	3.2	0.6501200	0.00121	15.4
	−0.4	0.8257064	0.022	3.3	0.6656460	0.00113	14.6
	−0.3	0.8193304	0.023	3.4	0.6819316	0.00105	13.8
Number of nodes: 17618	−0.2	0.8112754	0.024	3.5	0.6990344	0.00096	12.9
	−0.1	0.8007800	0.026	3.7	0.7170174	0.00087	12.1
	0	0.7865340	0.029	4.0	0.7359500	0.00077	11.2
	0.1	0.7660910	0.033	4.4	0.7559101	0.00067	10.2
	0.2	0.7342848	0.039	5.1	0.7769820	0.00056	9.3
	0.3	0.6779864	0.050	6.2	0.7992634	0.00044	8.3
	0.4	0.5512136	0.075	8.9	0.8228612	0.00031	7.2
	0.45	0.4011860	0.107	12.2	0.8351899	0.00025	6.7
$p_I = 0.2$							
	−0.95	0.7108944	0.0147	5.3	0.4161275	0.000550	21.7
	−0.9	0.7090160	0.0149	5.3	0.4224520	0.000539	21.4
	−0.8	0.7048652	0.0151	5.4	0.4356960	0.000517	20.8
Number of elements: 5543	−0.7	0.7000812	0.0154	5.5	0.4497960	0.000493	20.2
	−0.6	0.6945110	0.0158	5.6	0.4648400	0.000468	19.5
	−0.5	0.6879420	0.0162	5.7	0.4809275	0.000442	18.8
	−0.4	0.6800814	0.0167	5.9	0.4981668	0.000413	18.1
	−0.3	0.6705037	0.0174	6.1	0.5166875	0.000384	17.3
Number of nodes: 16984	−0.2	0.6585802	0.0182	6.3	0.5366384	0.000352	16.5
	−0.1	0.6433258	0.0193	6.6	0.5581926	0.000318	15.6
	0	0.6231200	0.0208	7.0	0.5815500	0.000281	14.6
	0.1	0.5950842	0.0228	7.6	0.6069470	0.000242	13.6
	0.2	0.5535734	0.0259	8.4	0.6346644	0.000199	12.6
	0.3	0.4857991	0.0310	9.8	0.6650345	0.000154	11.4
	0.4	0.3553004	0.0410	12.6	0.6984572	0.000105	10.1
	0.45	0.2311271	0.0512	15.4	0.7164610	0.000080	9.5
$p_I = 0.3$							
	−0.95	0.5957412	0.00847	6.5	0.3126325	0.0001157	19.7
	−0.9	0.5935440	0.00854	6.5	0.3182410	0.0001138	19.5
	−0.8	0.5886972	0.00870	6.6	0.3300860	0.0001100	19.1
Number of elements: 5638	−0.7	0.5831474	0.00887	6.7	0.3428460	0.0001061	18.7
	−0.6	0.5767194	0.00908	6.8	0.3566312	0.0001021	18.2
	−0.5	0.5691900	0.00931	6.9	0.3715725	0.0000979	17.7

(*continued*)

	ν_o	K^*/K_o	me K^* (%)	d_{K^*} (%)	G^*/G_o	me G_T^* (%)	$d_{G_T^*}$ (%)
	−0.4	0.5602500	0.00958	7.1	0.3878202	0.0000937	17.2
	−0.3	0.5494630	0.00991	7.3	0.4055541	0.0000892	16.6
Number of nodes: 17293	−0.2	0.5361888	0.01030	7.5	0.4249872	0.0000846	16.0
	−0.1	0.5194573	0.01078	7.8	0.4463766	0.0000797	15.3
	0	0.4977150	0.01139	8.2	0.4700330	0.0000746	14.6
	0.1	0.4683114	0.01219	8.7	0.4963376	0.0000693	13.7
	0.2	0.4263343	0.01329	9.5	0.5257596	0.0000635	12.8
	0.3	0.3615238	0.01498	10.6	0.5588908	0.0000575	11.8
	0.4	0.2482914	0.01809	12.8	0.5964784	0.0000513	10.7
	0.45	0.1526618	0.02133	14.6	0.6172346	0.0000488	10.1
$p_I = 0.4$							
	−0.95	0.4945472	0.028	6.6	0.2384230	0.00181	16.5
	−0.9	0.4922680	0.028	6.7	0.2431710	0.00179	16.4
	−0.8	0.4872592	0.029	6.7	0.2532600	0.00174	16.1
Number of elements: 5156	−0.7	0.4815425	0.030	6.8	0.2642208	0.00169	15.9
	−0.6	0.4749580	0.030	6.9	0.2761740	0.00163	15.6
	−0.5	0.4672890	0.031	7.0	0.2892595	0.00157	15.2
	−0.4	0.4582472	0.032	7.1	0.3036474	0.00150	14.9
	−0.3	0.4474243	0.033	7.3	0.3195409	0.00142	14.5
Number of nodes: 15813	−0.2	0.4342397	0.035	7.5	0.3371904	0.00133	14.1
	−0.1	0.4178228	0.037	7.7	0.3569040	0.00124	13.6
	0	0.3968200	0.039	8.0	0.3790650	0.00113	13.1
	0.1	0.3689972	0.043	8.4	0.4041609	0.00100	12.5
	0.2	0.3303893	0.047	9.0	0.4328148	0.00086	11.8
	0.3	0.2732174	0.055	9.8	0.4658420	0.00069	11.0
	0.4	0.1798518	0.067	11.2	0.5043262	0.00049	10.2
	0.45	0.1068359	0.078	12.3	0.5260557	0.00039	9.7
$p_I = 0.5$							
	−0.95	0.4018327	0.0082	6.1	0.1802985	0.000245	13.2
	−0.9	0.3996440	0.0082	6.2	0.1841690	0.000241	13.1
	−0.8	0.3948448	0.0083	6.2	0.1924320	0.000235	13.0
Number of elements: 4747	−0.7	0.3893897	0.0085	6.3	0.2014710	0.000228	12.8
	−0.6	0.3831344	0.0086	6.3	0.2114008	0.000220	12.6
	−0.5	0.3758880	0.0088	6.4	0.2223605	0.000212	12.4
	−0.4	0.3673955	0.0090	6.5	0.2345184	0.000203	12.2
	−0.3	0.3573046	0.0093	6.6	0.2480828	0.000103	12.0
Number of nodes: 14634	−0.2	0.3451168	0.0096	6.8	0.2633128	0.000182	11.7
	−0.1	0.3301042	0.0100	6.9	0.2805354	0.000170	11.4
	0	0.3111550	9.0106	7.1	0.3001680	0.000156	11.1
	0.1	0.2864866	0.0113	7.4	0.3227554	0.000141	10.7
	0.2	0.2530498	0.0123	7.8	0.3490188	0.000123	10.2
	0.3	0.2051608	0.0137	8.3	0.3799354	0.000103	9.7
	0.4	0.1308639	0.0161	9.2	0.4168612	0.000081	9.0
	0.45	0.0758949	0.0181	9.8	0.4381538	0.000071	8.7
$p_I = 0.6$							
	−0.95	0.31489795	0.028	5.3	0.13263000	0.00210	10.1
	−0.9	0.31293360	0.028	5.3	0.13564700	0.00208	10.0
	−0.8	0.30864132	0.028	5.3	0.14211180	0.00204	10.0
Number of elements: 5159	−0.7	0.30377880	0.029	5.3	0.14922390	0.00200	9.9
	−0.6	0.29822672	0.029	5.4	0.15708520	0.00195	9.8
	−0.5	0.29182600	0.030	5.4	0.16582100	0.00189	9.7
	−0.4	0.28436724	0.031	5.5	0.17558580	0.00183	9.5
	−0.3	0.27556256	0.032	5.6	0.18657240	0.00176	9.4
Number of nodes: 15910	−0.2	0.26501328	0.033	5.7	0.19902560	0.00168	9.2
	−0.1	0.25214328	0.034	5.8	0.21326040	0.00158	9.1
	0	0.23609200	0.036	5.9	0.22968800	0.00147	8.8
	0.1	0.21551288	0.038	6.1	0.24885740	0.00134	8.6
	0.2	0.18817560	0.042	6.3	0.27151920	0.00118	8.3
	0.3	0.15009696	0.046	6.6	0.29872050	0.00098	8.0
	0.4	0.09339820	0.054	7.1	0.33197920	0.00075	7.6
	0.45	0.05320384	0.061	7.4	0.35154815	0.00061	7.3

(*continued*)

	ν_o	K^*/K_o	me K^* (%)	d_{K^*} (%)	G^*/G_o	me G_T^* (%)	$d_{G_T^*}$ (%)
$p_I = 0.7$							
	−0.95	0.23204785	0.0051	4.2	0.09236250	0.000153	7.2
	−0.9	0.23042740	0.0051	4.2	0.09456310	0.000152	7.2
	−0.8	0.22689264	0.0051	4.2	0.09929500	0.000149	7.1
Number of elements: 5945	−0.7	0.22290336	0.0052	4.2	0.10452540	0.000146	7.1
	−0.6	0.21836584	0.0053	4.2	0.11033720	0.000142	7.1
	−0.5	0.21315900	0.0054	4.3	0.11683400	0.000138	7.0
	−0.4	0.2071234	0.0055	4.3	0.12414300	0.000134	7.0
	−0.3	0.2004208	0.0057	4.3	0.13242810	0.000129	6.9
Number of nodes: 18370	−0.2	0.19161968	0.0059	4.4	0.14189760	0.000123	6.8
	−0.1	0.18143460	0.0061	4.4	0.15282630	0.000117	6.7
	0	0.16886800	0.0064	4.5	0.16557800	0.000109	6.6
	0.1	0.15297568	0.0068	4.6	0.18065190	0.000100	6.5
	0.2	0.13223376	0.0073	4.7	0.19874520	0.000090	6.3
	0.3	0.10402444	0.0080	4.9	0.22086740	0.000077	6.1
	0.4	0.06343036	0.0092	5.1	0.24852940	0.000062	5.9
	0.45	0.03562549	0.0102	5.3	0.26513250	0.000054	5.8
$p_I = 0.8$							
	−0.95	0.15239210	0.0046	2.9	0.05760600	0.000098	4.6
	−0.9	0.1512187	0.0046	2.9	0.05903250	0.000097	4.6
	−0.8	0.14866436	0.0046	2.9	0.06210840	0.000095	4.6
Number of elements: 5714	−0.7	0.14579136	0.0046	2.9	0.06552240	0.000093	4.5
	−0.6	0.14253536	0.0047	2.9	0.06933360	0.000091	4.5
	−0.5	0.13881600	0.0047	2.9	0.07361550	0.000089	4.5
	−0.4	0.13452480	0.0048	2.9	0.07846140	0.000086	4.5
	−0.3	0.12952128	0.0048	2.9	0.08399020	0.000084	4.4
Number of nodes: 17789	−0.2	0.12360880	0.0049	3.0	0.09035680	0.000082	4.4
	−0.1	0.11651688	0.0050	3.0	0.09776790	0.000079	4.4
	0	0.10785500	0.0052	3.0	0.10650300	0.000076	4.3
	0.1	0.09703408	0.0054	3.1	0.11695310	0.000074	4.3
	0.2	0.08313264	0.0056	3.1	0.12967680	0.000070	4.2
	0.3	0.06461832	0.0060	3.2	0.14550640	0.000067	4.1
	0.4	0.03873716	0.0067	3.3	0.16573760	0.000064	4.0
	0.45	0.02150800	0.0075	3.3	0.17812090	0.000063	4.0
$p_I = 0.9$							
	−0.95	0.07521498	0.021	1.5	0.02710925	0.00138	2.2
	−0.9	0.07458332	0.021	1.5	0.02780280	0.00137	2.2
	−0.8	0.07321184	0.021	1.5	0.02930220	0.00134	2.2
Number of elements: 2518	−0.7	0.07167391	0.021	1.5	0.03097230	0.00132	2.2
	−0.6	0.06993791	0.021	1.5	0.03284460	0.00129	2.2
	−0.5	0.06796250	0.021	1.5	0.03495770	0.00127	2.2
	−0.4	0.06569467	0.022	1.5	0.03736140	0.00124	2.2
	−0.3	0.06306418	0.022	1.5	0.04012001	0.00121	2.2
Number of nodes: 8111	−0.2	0.05907645	0.022	1.5	0.04331856	0.00118	2.2
	−0.1	0.05630105	0.023	1.5	0.04707117	0.00115	2.1
	0	0.05185260	0.023	1.5	0.05153570	0.00112	2.1
	0.1	0.04635822	0.024	1.5	0.05693589	0.00108	2.1
	0.2	0.03940013	0.024	1.5	0.06360024	0.00105	2.1
	0.3	0.03030352	0.026	1.5	0.07203144	0.00101	2.1
	0.4	0.01790323	0.027	1.6	0.08303974	0.00097	2.1
	0.45	0.00984560	0.030	1.6	0.08991015	0.00096	2.0

References

[1] Ave llaneda M. Optimal bounds and microgeometries for elastic composites. SIAM J Appl Math 1987:1216–28.

[2] Berggren SA, Lukkassen D, Meidell A, Simula L. Some methods for calculating stiffness properties of periodic structues. To appear in Appl. Math.

[3] Bullen PS, Mitrinović DS, Vasić PM. Means and their inequalities. Dordrecht: Reidel, 1988.

[4] Bensøe MP. Optimization of structural topology, shape, and material. Berlin: Springer, 1995.

[5] Byström J, Jekabsons N, Varna J. An evaluation of different models for prediction of elastic properties of woven composites. Composites: Part B 2000;31:7–20.

[6] Zienkiewicz OC, Zhu JZ. A simple error estimator and adaptive procedure for practical engineering analysis. Int J Numer Meth Engng 1987;24:337–57.
[7] Francfort GA, Murat F. Homogenization and optimal bounds in linear elasticity. Arch Rational Mech Anal 1986;94:307–34.
[8] Gibiansky LV. Bounds on effective moduli of composite materials. Lecture Notes. School on Homogenization, ICTP, Trieste, 1993.
[9] Gibson LJ, Ashby MF. Cellular solids. Cambridge: Cambridge University Press, 1997.
[10] Greengard L, Helsing J. On the numerical evaluation of elastostatic fields in locally isotropic two-dimensional composites. J Mech Phys Solids 1998;46:1441–62.
[11] Hashin Z. Analysis of composite materials — a survey. J Appl Mech 1983;50:481–505.
[12] Helsing J, Jonsson A. Elastostatics for plates with holes, Department of Solid Mechanics, KTH Research Report TRITA-HLF-0250, 1999.
[13] Hill R. Theory of mechanical properties of fibre-strengthened materials. I. Elastic behaviour. J Mech Phys Solids 1964;12:199–212.
[14] Holmbom A, Persson L-E, Svanstedt N. A homogenization procedure for computing effective moduli and microstresses in composite materials. J Compos Engng 1992;2(4):249–59.
[16] Jikov VV, Kozlov SM, Oleinik OA. Homogenization of differential operators and integral functionals. Berlin: Springer, 1994.
[17] Lakes R. Materials with structural hierarchy. Nature 1993;361:511–5.
[19] Lukkassen D. A new reiterated structure with optimal macroscopic behavior. SIAM J Appl Math 1999;59(5):1825–42.
[20] Lukkassen D, Persson L-E, Wall P. Some engineering and mathematical aspects on the homogenization method. Compos Engng 1995;5(5):519–31.
[21] Meidell A. The out-of-plane shear modulus of two-component regular honeycombs with arbitrary thickness. In: Mota Soares CA, Mota Soares CM, Freitas MJM, editors. Mechanics of composite materials and structures, vol. III. Troia, Portugal: NATO ASI, 1998. p. 367–79.
[22] Meidell A, Wall P. Homogenization and design of structures with optimal macroscopic behaviour. In: Hernández S, Breddia CA, editors. Computer aided optimum design of structures V, Southampton: Computational Mechancis Publications, 1997. p. 393–402.
[23] Milton G. Composite materials with Poisson's ratio close to −1. J Mech Phys Solids 1992;49:1105–37.
[24] Persson L-E, Persson L, Svanstedt N, Wyller J. The homogenization method: an introduction. Lund: Studentlitteratur, 1993.